J. Vis. Commun. Image R. 35 (2016) 193–197

Contents lists available at ScienceDirect

J. Vis. Commun. Image R.

journal homepage: www.elsevier.com/locate/jvci

Short Communication

Halftoning-based Block Truncation Coding image restoration ☆

Jing-Ming Guo [a,*], Heri Prasetyo [a], KokSheik Wong [b]

[a] Department of Electrical Engineering, National Taiwan University of Science and Technology, Taipei, Taiwan
[b] Faculty of Computer Science and Information Technology, University of Malaya, Kuala Lumpur, Malaysia

ARTICLE INFO

Article history:
Received 20 August 2015
Accepted 28 December 2015
Available online 4 January 2016

Keywords:
Halftoning
Error diffusion
Ordered dithering
Block truncation coding
Image restoration
Sparse representation
Image compression
Vector quantization

ABSTRACT

This paper presents a new image restoration method for improving the quality of halftoning-Block Truncation Coding (BTC) decoded image in a patch-based manner. The halftoning-BTC decoded image suffers from the halftoning impulse noise which can be effectively reduced and suppressed using the Vector Quantization (VQ)-based and sparsity-based approaches. The VQ-based approach employs the visual codebook generated from the clean image, whereas the sparsity-based approach utilizes the double learned dictionaries in the noise reduction. The sparsity-based approach assumes that the halftoning-BTC decode image and clean image share the same sparsity coefficient. In the sparse coding stage, it uses the halftoning-BTC dictionary, while in the reconstruction stage, it exploits the clean image dictionary. As suggested by the experimental results, the proposed method outperforms in the halftoning-BTC image reconstructed when compared to that of the filtering approaches.

1. Introduction

Halftoning Block Truncation Coding (BTC) is an image compression method, which requires simple process for both the encoding and decoding stages. It compresses an image by dividing an input image into several image blocks, where each image block is subsequently represented by two quantization values and a bitmap image. The decoding process performs the reverse procedure by simply replacing the bitmap information with the high or low quantization values. Several improvements and enhancements of this image compression scheme are reported in literature [1,2,5] to further reduce the computational complexity, improve image quality, and achieve higher compression ratio.

The dithering-based BTC, namely Ordered Dither Block Truncation Coding (ODBTC) [1,2], and diffused-based BTC, called Error Diffusion Block Truncation Coding (EDBTC) [5] exploit the low-pass nature of the Human Visual System (HVS) for achieving an acceptable perceptual image quality. These methods replace the classical bitmap image with the halftone image. Given the high efficiency and low computational complexity of the ODBTC, some interesting applications are developed, including watermarking schemes [3] and content-based image retrieval [4]. The attractive properties of EDBTC then led to its deployment in several applications, including image watermarking [6], data hiding [7], and content-based image retrieval [8].

Despite their benefits and superior performances, ODBTC and EDBTC as well as their applications usually consider only the reconstructed image, but without image restoration for enhancement purpose.

To improve image quality, a restoration technique on the halftoning-based Block Truncation Coding (BTC) is proposed. Some halftoning-based BTC methods have been recently proposed: Guo et al. [9] employed the OD/ED BTC with the optimized classified filter set to remove the impulse noises. In this work, the image patch processing approaches are utilized: (1) The Vector Quantization (VQ)-based technique uses a set of clean images to obtain the representative visual codebook. (2) The sparsity-based technique uses a set of clean images and their corresponding halftoning-BTC decoded images to learn two representative dictionaries. These two techniques, which utilize codebook and dictionaries, lead to good image quality. Yet, the impulse noises are still differentiable. Thus, this study, we try to further improve image quality in terms of this issue.

The rest of this paper is organized as follows. The related work for image restoration of halftoning-BTC reconstructed image is briefly reviewed in Section 2. Section 3 elaborates on the image patch image restoration of halftoning-BTC decoded image. Experimental results are reported in Section 4. Finally, conclusions are drawn in Section 5.

☆ This paper has been recommended for acceptance by Zicheng Liu.

* Corresponding author.
E-mail addresses: jmguo@seed.net.tw (J.-M. Guo), heri_inf_its_02@yahoo.co.id (H. Prasetyo), koksheik@um.edu.my (K. Wong).

http://dx.doi.org/10.1016/j.jvcir.2015.12.016
1047-3203/

2. Related work

This section briefly reviews two halftoning-BTC methods, namely ODBTC [1] and EDBTC [5]. The related work on halftoning-BTC image restoration is also presented. Two filtering processes assuming that the halftoning-BTC decoded image is corrupted with additional noise are also presented, where the filtering approaches are conducted to suppress this noise for obtaining better image quality.

2.1. Halftoning-BTC

The halftoning-BTC methods, including ODBTC and EDBTC, convert a continuous tone image into another representation with lower bit requirement, which can be illustrated by the schematic diagram shown in Fig. 1. Let I be an image of size $M \times N$, which is then divided into non-overlapping blocks $i(x,y)$ each of size $m \times n$. Each image block is further represented by two extreme quantization values and the bitmap image as follows:

$$\mathcal{H}\{i(x,y)\} \Rightarrow \{q_{min}, q_{max}, bm(x,y)\}, \tag{1}$$

where q_{min} and q_{max} denote the two extreme quantization values, and $bm(x,y)$ represents the corresponding bitmap image. The quantization values can be simply obtained by searching the minimum and maximum pixel values within the image block defined as follows:

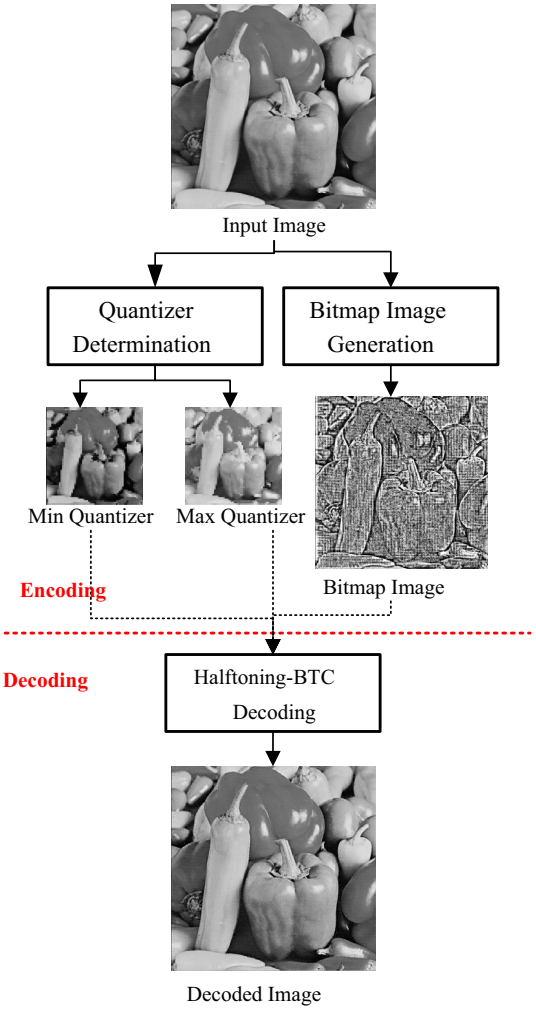

Fig. 1. Schematic diagram of halftoning-BTC image compression.

$$q_{min} = \min_{\forall x,y} \{i(x,y)\}, \tag{2}$$

$$q_{max} = \max_{x,y} \{i(x,y)\}, \tag{3}$$

for $x = 1,2,\ldots,m$ and $y = 1,2,\ldots,n$. Both ODBTC and EDBTC employ the same extreme quantization values, but the main difference between ODBTC and EDBTC is in the bitmap image generation process. Specifically, to generate the bitmap image, ODBTC utilizes a dither array that has the same size as the image block, while EDBTC exploits an error kernel.

Let $D(x,y)$ be a dither array of the same size as the image block, i.e., $m \times n$. The scaled version of this dither array $\{D^0, D^1, \ldots, D^{255}\}$ can be pre-calculated offline to reduce the computational time [2]. The ODBTC bitmap can be obtained by using the following thresholding method:

$$bm(x,y) = \begin{cases} 1, & \text{if } i(x,y) \geqslant q_{min} + D^d(x,y); \\ 0, & \text{otherwise}, \end{cases} \tag{4}$$

where $d = q_{max} - q_{min}$. On the other hand, the EDBTC bitmap image can be computed by incorporating the error kernel ϵ such as the Floyd–Steinberg kernel. The thresholding operation for EDBTC bitmap image is formally defined as

$$bm(x,y) = \begin{cases} 1, & \text{if } i(x,y) \geqslant \tilde{i}; \\ 0, & \text{otherwise}, \end{cases} \tag{5}$$

where $\tilde{i}$ denotes the mean value of all pixels in the image block. The error value obtained from this thresholding operation is further diffused into its neighboring pixels by means of the error kernel as follows:

$$i(x,y) \leftarrow i(x,y) + e(x,y) \times \epsilon, \tag{6}$$

where $e(x,y)$ is the error after the thresholding operation. Interested reader is referred to Refs. [1,2,5] for the detailed descriptions on ODBTC and EDBTC image compression techniques.

The two quantization values and the bitmap image are then transmitted to the decoder, which simply replaces the bitmap image of value 1 with the max, quantization value, and vice versa. The decoding process of ODBTC and EDBTC can be performed using the following step:

$$o(x,y) = \begin{cases} q_{max}, & \text{if } bm(x,y) = 1; \\ q_{min}, & \text{otherwise}. \end{cases} \tag{7}$$

The decoding process on halftoning-BTC is very simple, making it very suitable for real time application.

2.2. Lowpass filtering image restoration

The image reconstructed by halftoning-BTC often contains the halftoning impulse noise, making it less pleasant for human vision. To improve quality, image restoration can be performed on the halftoning-BTC decoded image. A naïve approach is to apply lowpass filtering [9]. Hereinafter, the Gaussian filter is exploited to suppress the halftoning noise as well as removing the blocking effect and false contour. Let $O(x,y)$ be the halftoning-BTC decoded image. The Gaussian lowpass filtering with μ and σ^2 is defined as

$$\widetilde{R}(x,y) = O(x,y) * f_{\mu,\sigma^2}(x,y), \tag{8}$$

for $x = 1,2,\ldots,M$ and $y = 1,2,\ldots,N$, where $\widetilde{R}(x,y)$ denotes the reconstructed image after applying the Gaussian lowpass filter.

2.3. Variance classified filtering image restoration

The lowpass filter may yield unsatisfactory reconstructed image since it changes the characteristic and statistics of the image in a uniform manner, while different image block requires different treatment to obtain better quality. Thus, the variance classified filtering [9] is designed to offer an alternative way for performing lowpass filtering by incorporating different filter set in the halftoning-BTC reconstructed image. Let $T = \{i_k(x,y), o_k(x,y)\}$ be a training set consisting of K images, for $k = 1,2,\ldots,K$. Let $i_k(x,y)$ and $o_k(x,y)$ denote the original and halftoning-BTC decoded image, respectively. A set of variance classified filters can be computed from this training image to obtain $F = \{f_{\sigma_1^2}(x,y), f_{\sigma_2^2}(x,y), \ldots, f_{\sigma_n^2}(x,y)\}$, i.e., a set of lowpass filters with different kernel coefficient that depends on the variance value.

This set of filters can be iteratively calculated from a set of training images as a minimization problem formulated as follows:

$$\min_{f_{\sigma^2}(x,y)} \|i_k(x,y) - o_k(x,y) * f_{\sigma^2}(x,y)\|_2^2. \tag{9}$$

The halftoning-BTC decoded image can be subsequently reconstructed by using the following equation:

$$\widetilde{R}(x,y) = O(x,y) * f_{\sigma^2}(x,y), \tag{10}$$

for $x = 1,2,\ldots,M$ and $y = 1,2,\ldots,N$. Given an image block, the suitable kernel is chosen based on the variance of the block for performing the filtering process.

3. Proposed halftoning-BTC image restoration

This section proposes two image restoration methods on reconstructed halftoning-BTC image. These two techniques share the same methodology by exploiting the image patch processing and using clean images (i.e., without noise) for training. The first method is the Vector Quantization (VQ)-based image restoration, while the second method is the sparsity-based image restoration. These methods exploit a set of clean images for generating the representative codebook. Using these strategies, quality of the halftoning-BTC decoded image can be improved by incorporating the clean images.

3.1. VQ-based image restoration

In this image restoration method, a set of clean images are required to obtain the representative visual codebook. Fig. 2 shows the schematic diagram of VQ-based image restoration for improving the quality of halftoning-BTC decoded image. Let $T = \{i_k(x,y)\}$ be a set of clean images. This image set can be regarded as the training set. The VQ-based image restoration produces a set of representative visual codebook $C = \{C_1, C_2, \ldots, C_{N_c}\}$ containing N_c codewords from the training set. The visual codebook can be generated by applying the K-means clustering on the training image set.

In the halftoning-BTC reconstructed image, the decoded image patch $o(x,y)$ is firstly matched with the visual codebook based with the lowest distortion, which can be simply computed as follows:

$$c^* = \arg\min_{c=1,2,\ldots,N_c} \{\|o(x,y) - C_c\|_2^2\}. \tag{11}$$

Therefore, c^* denotes the codeword index which yields the smallest difference for the image patch $o(x,y)$. The image patch $o(x,y)$ is subsequently replaced by the codeword C_{c^*} as follows:

$$\tilde{o}(x,y) = C_{c^*}, \tag{12}$$

where $\tilde{o}(x,y)$ denotes the reconstructed image patch at position (x,y). Since the problem in (12) is overdetermined, the halftoning-BTC reconstructed image can be later obtained by averaging the image patches as follows:

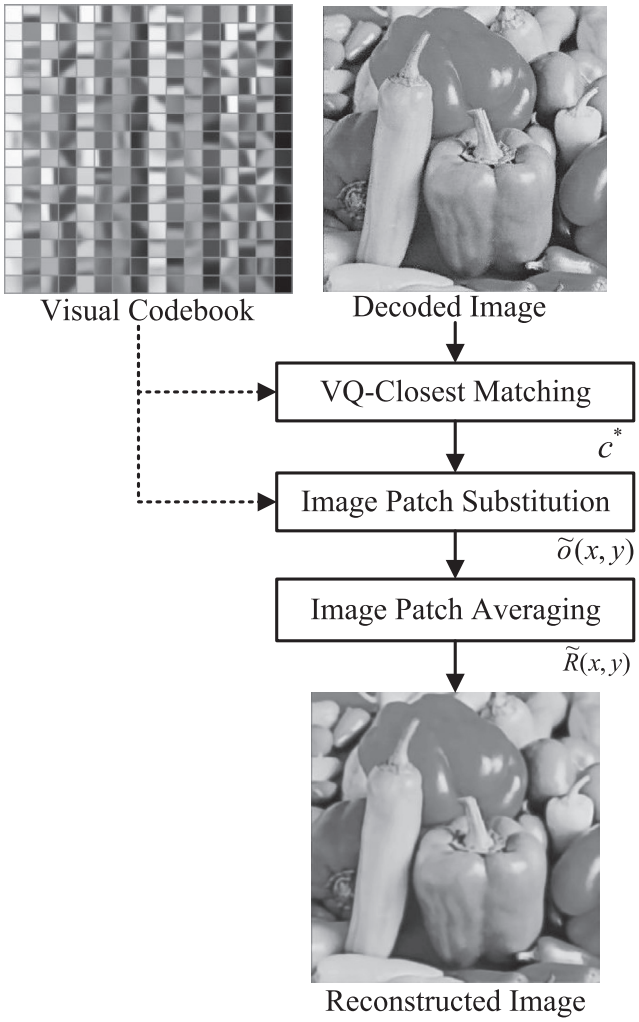

Fig. 2. Schematic diagram of VQ-based image restoration.

$$\widetilde{R}(x,y) = \frac{\sum \tilde{o}(x,y)}{\sum R(x,y)^T R(x,y)}, \tag{13}$$

where $R(x,y)$ is the image patch extraction operator [11].

3.2. Sparsity-based image restoration

In sparsity-based image restoration, a set of clean images and their corresponding halftoning-BTC decoded images are needed to obtain the representative learned dictionaries. Fig. 3 depicts the schematic diagram of sparsity-based image restoration, which incorporates two learned dictionaries, i.e., one dictionary from the halftoning-BTC decoded image and another dictionary from the clean image. Let $T = \{i_k(x,y), o_k(x,y)\}$ be a training set consisting of K clean images $i_k(x,y)$ and their corresponding halftoning-BTC images $o_k(x,y)$ for $k = 1,2,\ldots,K$. Two dictionaries, namely the clean image dictionary D^c and haltone-BTC image dictionary D^h, can be computed and trained from the set of images as follows:

$$\min_{D^c,D^h,\alpha} \{\|i - D^c\alpha\|_2^2 + \|o - D^h\alpha\|_2^2\} + \lambda\|\alpha\|_1, \tag{14}$$

where α and λ denote the sparse representation and the sparse regularization term, respectively. Since both dictionaries employ the same sparse representation, the problem in (14) can be expressed as

$$\min_{D,\alpha} \{\|Y - D\alpha\|_2^2\} + \lambda\|\alpha\|_1, \tag{15}$$

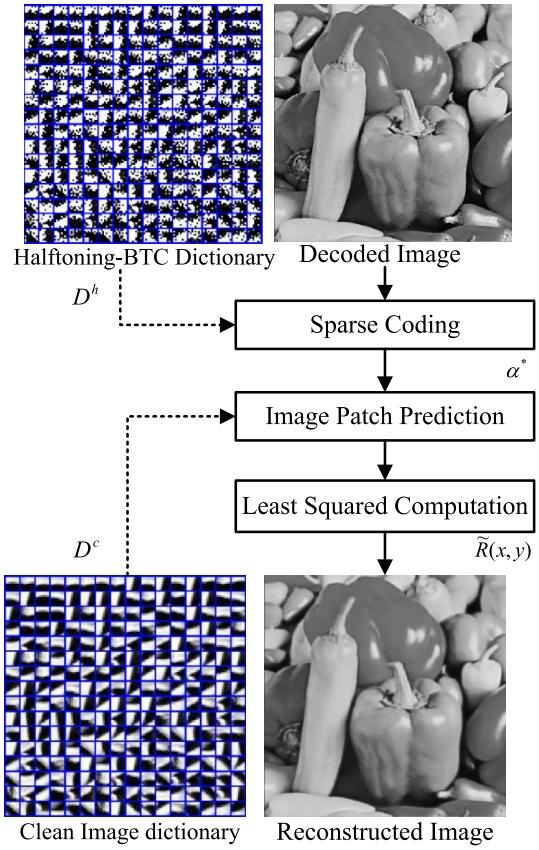

Fig. 3. Schematic diagram of sparsity-based image restoration.

where $Y = [i^T, o^T]^T$ is the concatenation of clean image patch and its corresponding halftoning-BTC image patch. The dictionary D is then defined as $D = [D^c; D^h]$, i.e., the concatenation of clean image dictionary and halftoning-BTC image dictionary. The optimization problem in (15) can be solved using the KSVD [10], which has been found to be effective in noise removal [11], compressive sensing [12], image super-resolution [13], etc., as well as other dictionary learning algorithms.

In the sparse coding stage, the sparse coefficient is first computed from the halftoning-BTC image patch $o(x,y)$ and the halftoning-BTC image dictionary D^h as follows:

$$\min_{\alpha^*}\{\|o(x,y) - D^h\alpha\|_2^2\} + \lambda\|\alpha\|_1. \tag{16}$$

The optimum sparse coefficient can be predicted using the Orthogonal Matching Pursuit (OMP) algorithm or other matching pursuit approximation. The halftoning-BTC reconstructed image patch $\widetilde{R}(x,y)$ can be subsequently obtained from the clean image dictionary D^c with the optimum sparse coefficient α^* as follows:

$$\min_{\widetilde{R}(x,y)}\{\|R(x,y)\widetilde{R}(x,y) - D^c\alpha^*\|_2^2\}, \tag{17}$$

where $\widetilde{R}(x,y)$ is the halftoning-BTC reconstructed image. Since the optimization in (17) is simply the least squared problem, the solution for (17) is then trivially given as

$$\widetilde{R}(x,y) = \left\{\sum R(x,y)^T R(x,y)\right\}^{-1} \sum R(x,y)^T D^c\alpha^*, \tag{18}$$

where $R(x,y)$ denotes the patch extraction operator. The formulation in (18) is similar to the averaging operation on the VQ-based image restoration. By using the overcomplete dictionaries computed from the clean images and the halftoning-BTC images, halftoning-BTC decoded image of higher quality can be obtained.

4. Experiments

Experiments were conducted using the same natural images (i.e., 40 in total) as considered in [9]. These images are split into the training and testing sets. The variance classified filtering, VQ-based, and sparsity-based methods employ the training set for obtaining the optimal filter sets, the optimal visual codebook, and the optimal dictionaries, respectively. Throughout the discussion, the image quality comparison between the original and reconstructed image is measured in terms of Peak-Signal–Noise-Ratio (PSNR). The image block size for both ODBTC and EDBTC are set at 8×8 and 16×16 for experiment purpose.

4.1. ODBTC and EDBTC image restoration

This subsection compares the quality achieved by the filtering-based and patch-based methods on ODBTC and EDBTC reconstructed image. In this experiment, the block size considered for ODBTC and EDBTC is 8×8. To suppress the halftoning impulse noise, the lowpass filtering considers the Gaussian kernel of size 9×9 with $\mu = 0$ and $\sigma = 1$, while the variance classified filtering utilizes 13 optimized kernels of size 7×7. The VQ-based and sparsity-based methods exploit 1024 optimal visual codebooks and 1024 optimal atoms in the learned dictionary, respectively. The image patch for VQ-based and sparsity-based methods is set at 8×8.

For visual inspection, Fig. 4 shows the image "Lake" reconstructed from ODBTC and EDBTC, coupled with various image restoration methods. The first column shows without image restoration image. The second column shows the variance classified filtering method. The rest of column depicts the output of VQ-based and sparsity-based image restoration methods, respectively.

4.2. Performance comparison

This subsection compares the performance of various image restoration methods when applied on the ODBTC and EDBTC reconstructed images. The same experiment setup is considered, while the performance comparison is conducted under ODBTC and EDBTC using block sizes of 8×8 and 16×16. Table 1 records the average PSNR (SSIM) value of 20 images. Based on the results, the ODBTC image restoration improves the image quality as indicated by its higher PSNR (SSIM) value when compared to the case without image restoration. Note that variance classified filtering achieves higher reconstructed image quality when compared to that of lowpass filtering because it employs the training set for obtaining the optimum kernel coefficient. Nonetheless, the sparsity-based approach yields the best image quality because it employs the clean image for obtaining the optimum dictionary. Notably, an average improvement of >5 dB is observed when compared to lowpass filtering and variance classified filtering methods in [9].

Similarly, Table 1 also suggests that the sparsity-based approach yields the best image quality when compared to the other schemes under EDBTC, with an average improvement of >3 dB when compared to [9]. Thus, the sparsity-based image reconstruction can be regarded as a good candidate for improving the quality of ODBTC and EDBTC reconstructed images.

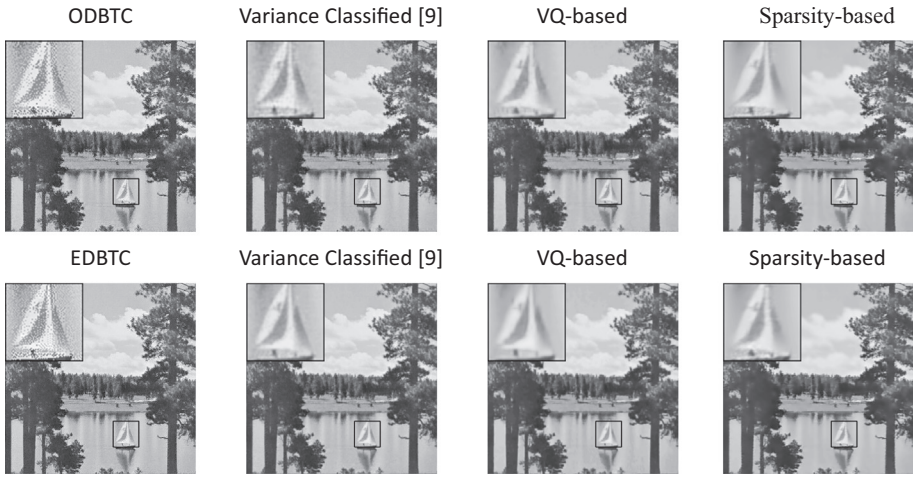

Fig. 4. Comparison of image quality for ODBTC (1st row) and EDBTC (2nd row).

Table 1
Average PSNR (dB) and SSIM of 20 test images for various image restoration methods.

	ODBTC		EDBTC	
	8×8	16×16	8×8	16×16
Method (PSNR)				
(a) PSNR				
Without image restoration	19.23	16.10	20.14	16.54
Lowpass filtered [9]	29.14	28.46	30.76	30.11
Variance classified [9]	29.48	28.63	31.63	30.82
VQ-based	33.92	33.85	34.15	34.10
Sparsity-based	**34.50**	**34.33**	**34.82**	**34.70**
Method (SSIM)				
(b) SSIM				
Without image restoration	0.884	0.800	0.907	0.821
Lowpass filtered [9]	0.980	0.978	0.985	0.984
Variance classified [9]	0.982	0.979	0.989	0.987
VQ-based	0.995	0.994	0.996	0.996
Sparsity-based	**0.996**	**0.996**	**0.997**	**0.997**

5. Conclusions

Two new methods for improving the reconstructed image quality from the Ordered Dither and Error Diffusion Block Truncation Coding (ODBTC and EDBTC) are proposed in this paper. The decoded image from ODBTC and EDBTC are first regarded as noisy image. The VQ-based and sparsity-based image restoration then suppresses the halftoning impulse noise from the ODBTC and EDBTC decoded images in patch-based manner. Experimental results suggest that the proposed method yields better reconstructed image quality when compared to the former image restoration approaches, including lowpass filtering and variance classified filtering. This improvement suggests that the halftoning-based BTC schemes can be regarded as a potential candidate in image compression and computer vision applications.

References

[1] J.M. Guo, M.F. Wu, Improved block truncation coding based on the void-and-cluster dithering approach, IEEE Trans. Image Process. 18 (1) (2009) 211–213.
[2] J.M. Guo, High efficiency ordered dither block truncation with dither array LUT and its scalable coding application, Dig. Signal Process. 20 (1) (2010) 97–110.
[3] J.M. Guo, M.F. Wu, Y.C. Kang, Watermarking in conjugate ordered dither block truncation coding images, Sig. Process. 89 (10) (2009) 1864–1882.
[4] J.M. Guo, H. Prasetyo, Content-based image retrieval using features extracted from halftoning-based block truncation coding, IEEE Image Process. 24 (3) (2015) 1010–1024.
[5] J.M. Guo, Improved block truncation coding using modified error diffusion, Electron. Lett. 44 (7) (2008).
[6] J.M. Guo, Y.F. Liu, Joint compression/watermarking scheme using majority-parity guidance and halftoning-based block truncation coding, IEEE Trans. Image Process. 19 (8) (2010) 2056–2069.
[7] J.M. Guo, Y.F. Liu, High capacity data hiding for error-diffused block truncation coding, IEEE Trans. Image Process. 21 (12) (2012) 4808–4818.
[8] J.M. Guo, H. Prasetyo, Content-based image retrieval using error diffusion block truncation coding features, IEEE Trans. Circuits Syst. Video Technol. 25 (3) (2015) 466–481.
[9] J.M. Guo, C.C. Su, H.J. Kim, Blocking effect and halftoning impulse suppression in an ED/OD BTC image with optimized texture-dependent filter sets, in: International Conference on System Science and Engineering (ICSSE 2011), Macau, China, June 2011, pp. 593–596.
[10] M. Aharon, M. Elad, A. Bruckstein, K-SVD: an algorithm for designing overcomplete dictionaries for sparse representation, IEEE Trans. Signal Process. 54 (11) (2006) 4311–4322.
[11] M. Elad, M. Aharon, Image denoising via sparse and redundant representations over learned dictionaries, IEEE Trans. Image Process. 15 (12) (2006) 3736–3745.
[12] M. Xu, S. Li, J. Lu, W. Zhu, Compressibility constrained sparse representation with learnt dictionary for low bit-rate image compression, IEEE Trans. Circuits Syst. Video Technol. 24 (10) (2014) 1743–1757.
[13] J. Yang, J. Wright, T.S. huang, Y. Ma, Image super-resolution via sparse representation, IEEE Trans. Image Process. 19 (11) (2010).